Received: 10 March 2023 | Accepted: 4 July 2023

DOI: 10.1111/1365-2656.13990

Journal of Animal Ecology | BRITISH ECOLOGICAL SOCIETY

RESEARCH ARTICLE

Partitioning variance in population growth for models with environmental and demographic stochasticity

Jonas Knape[1] | Matthieu Paquet[1,2] | Debora Arlt[1,3] | Ineta Kačergytė[1] | Tomas Pärt[1]

[1]Department of Ecology, Swedish University of Agricultural Sciences, Uppsala, Sweden

[2]Institute of Mathematics of Bordeaux, University of Bordeaux, CNRS, Bordeaux INP, Talence, France

[3]SLU Swedish Species Information Centre, Swedish University of Agricultural Sciences, Uppsala, Sweden

Correspondence
Jonas Knape
Email: jonas.knape@slu.se

Funding information
Svenska Forskningsrådet Formas, Grant/Award Number: 2017-1064

Handling Editor: Fernando Colchero

Abstract

1. How demographic factors lead to variation or change in growth rates can be investigated using life table response experiments (LTRE) based on structured population models. Traditionally, LTREs focused on decomposing the asymptotic growth rate, but more recently decompositions of annual 'realized' growth rates using 'transient' LTREs have gained in popularity.
2. Transient LTREs have been used particularly to understand how variation in vital rates translate into variation in growth for populations under long-term study. For these, complete population models may be constructed to investigate how temporal variation in environmental drivers affect vital rates. Such investigations have usually come down to estimating covariate coefficients for the effects of environmental variables on vital rates, but formal ways of assessing how they lead to variation in growth rates have been lacking.
3. We extend transient LTREs to further partition the contributions from vital rates into contributions from temporally varying factors that affect them. The decomposition allows one to compare the resultant effect on the growth rate of different environmental factors, as well as density dependence, which may each act via multiple vital rates. We also show how realized growth rates can be decomposed into separate components from environmental and demographic stochasticity. The latter is typically omitted in LTRE analyses.
4. We illustrate these extensions with an integrated population model (IPM) for data from a 26 years study on northern wheatears (*Oenanthe oenanthe*), a migratory passerine bird breeding in an agricultural landscape. For this population, consisting of around 50–120 breeding pairs per year, we partition variation in realized growth rates into environmental contributions from temperature, rainfall, population density and unexplained random variation via multiple vital rates, and from demographic stochasticity.
5. The case study suggests that variation in first year survival via the unexplained random component, and adult survival via temperature are two main factors behind environmental variation in growth rates. More than half of the variation in

growth rates is suggested to come from demographic stochasticity, demonstrating the importance of this factor for populations of moderate size.

KEYWORDS
demographic stochasticity, environmental stochasticity, growth rate, integrated population model, life table response experiment

1 | INTRODUCTION

Populations in the wild regularly experience changes in their environments, resulting in variation in demographic rates such as survival, birth, immigration and emigration rates. Life table response experiments (LTREs) are a suite of methods developed with the aim of understanding how such change in demographic rates translate into variation or change in population growth (Caswell, 1989). The use of LTREs initially focused on decomposing changes in the asymptotic growth rate of stage or age structured deterministic matrix models into contributions from demographic rates and also from environmental factors determining those rates. In a frequently changing environment asymptotic growth rates may, however, never be attained as constant perturbations hinder the population from approaching the stable stage structure associated with any particular environmental state. In such dynamic environments, LTREs based on asymptotic growth rates may not accurately capture the demographic causes of variation. For instance, Koons et al. (2016) showed that the demographic factors highlighted as important in explaining variation in asymptotic growth rates by classical LTREs were not the same as those causing variation in the short term.

As an alternative, LTREs have been developed from stochastic matrix population models (Davison et al., 2013). These too study long-run asymptotic behaviour, but of the stochastic growth rate (Cohen, 1977) rather than of the deterministic growth rate of any particular environment. A more empirical approach is to base LTREs on the growth rate over a single time step and study how this 'realized' growth rate varies over a finite period of time such as the duration of a study. This was used by Brown et al. (1993), who derived exact decompositions of variation in realized growth rates into contributions from vital rates. Koons et al. (2016) instead defined 'transient LTREs' using Taylor approximations to decompose the variation in realized growth rates into contributions from vital rates and stage-structure. While these are called transient LTREs, they are not only useful in non-stationary environments or in a state away from equilibrium but also to analyse population variation in stationary stochastic environments.

LTREs have often been used as a theoretical tool to gain a deeper understanding of already parametrized population models but LTREs of realized growth rates also lend themselves well in an inferential context. One example is integrated population models (IPMs; Besbeas et al., 2005; Plard et al., 2019) that can be used to fit fairly complete structured population models by combining multiple types of demographic and population data. When such models include temporal variation in vital rates, they can be combined with transient LTREs to estimate contributions of variation in demographic vital rates to variation in population growth along with its uncertainty (Koons et al., 2017; Paquet et al., 2019).

Population models can further be used to investigate relations between temporal variation in environmental variables and variation in growth rates, mediated via demographic rates (Clark-Wolf et al., 2023; Weegman et al., 2017; Zhao et al., 2021). Such studies have usually used estimated covariate coefficients to assess the influence of environmental variables on demographic rates. A large coefficient does, however, not necessarily imply a large impact on the growth rate if the sensitivity of the vital rate is low. Similarly, opposing directions of effects of the same environmental variable on multiple vital rates can lead to unclear resultant effects on the growth rate (Canonne et al., 2023). Investigations into how environmental variation translates into variation in growth have been done with asymptotic LTREs (Caswell, 2001; Davison et al., 2013) but rarely with transient LTREs. An exception is Maldonado-Chaparro et al. (2018) who suggested regression on simulated population trajectories to decompose variation in annual growth into environmental contributions for integral projection models.

The aim of this paper is to explore a decomposition of variation in realized growth rates into contributions from environmental factors and density dependence acting via the vital rates, extending the methods of Koons et al. (2016). In addition, we propose an approach to quantify the relative contributions of environmental and demographic stochasticity to variation in growth rates. We apply these decompositions to an IPM of northern wheatears (*Oenanthe oenanthe*), where we include temperature and rainfall during different periods of the annual cycle, as well as breeding period density dependence, as explanatory covariates for vital rate variation.

2 | MATERIALS AND METHODS

2.1 | Scope

We consider a modelling framework where we have a structured population model with environmental variation and, possibly, demographic stochasticity. Environmental variation refers to temporal fluctuations in demographic rates across a population and demographic stochasticity to chance events of demographic outcomes for individuals (Engen et al., 1998). Environmental variation can be captured by projection matrices A_t for each time step t,

which are determined by a set of vital rates. Below, we will assume that t represents year, so that we have annual projection matrices. The vital rates determining the A_t matrices may vary over years and can be driven by environmental variables. In general, we think of the annual vital rates as modelled with some link function for an appropriate scale (e.g. logit for survival probabilities) and with a linear predictor that may include population level annual environmental covariates and random effects. We also include the possibility of simple density dependence, for example via total population size, in the linear predictors. This framework covers common types of models inferred via fitting IPMs (Schaub & Kéry, 2021).

2.2 | Contributions from population structure and environmental variation

We start by considering only environmental variation in population dynamics and decompose variation in realized growth rates into contributions from population structure (in terms of age or stage), density dependence and environmental factors. Later (Section 2.4), we will also consider demographic stochasticity.

Under environmental variation only, age or stage structured population dynamics are fully described in terms of the annual projection matrices A_t, and $n_{t+1} = A_t n_t$, where n_t is a vector containing the population numbers in the different ages or stages. The realized annual growth rate (as defined in Koons et al., 2016) is then

$$\lambda_t^{ES} = \frac{\| A_t n_t \|}{\| n_t \|} = \| A_t \tilde{n}_t \|,$$

where $\| \cdot \|$ is the *l1* vector norm (i.e. the total of all elements in the vector) and $\tilde{n}_t$ is the normalized population age or stage-structure vector. We use the superscript ES to highlight that this growth rate is determined by the state of the environment (A_t) and by the stage structure.

Koons et al. (2016) used a Taylor approximation of λ_t^{ES} to break down its variance $V(\lambda_t^{ES})$ into contributions from time varying vital rates. The same type of first order Taylor approximation is also commonly used for computing classical LTREs of deterministic asymptotic growth rates (Caswell, 2001). For these classical LTREs, the first order approximation has further been used to compute contributions from environmental factors acting on the vital rates. We use the same approach here but apply it to realized annual growth rates instead of deterministic asymptotic growth rates.

To help illustrate the approximation, we write the annual realized growth rate as a function of all its underlying time varying parameters:

$$\lambda_t^{ES} = f(\theta),$$

so that λ_t^{ES} is completely determined by θ. A first order Taylor expansion around the mean of θ gives

$$f(\theta) \approx f(\bar{\theta}) + \nabla f_{\bar{\theta}}^T \ (\theta - \bar{\theta}),$$

where $\nabla f_{\bar{\theta}} = \left(\frac{\partial f}{\partial \theta_1}\Big|_{\bar{\theta}}, \cdots, \frac{\partial f}{\partial \theta_k}\Big|_{\bar{\theta}} \right)$ is the gradient of f evaluated at the (temporal) mean of the vector θ, and T denotes vector transpose. Using rules for how to compute the variance of a vector of random parameters multiplied by a fixed vector, the variance of f can be approximated as

$$\mathrm{Var}(f(\theta)) \approx \nabla f_{\bar{\theta}}^T \ \Sigma_\theta \ \nabla f_{\bar{\theta}},$$

where Σ_θ is the covariance matrix of θ. This is identical to a delta approximation (Ver Hoef, 2012) for the variance of the function f given the covariance matrix of its parameters.

The formula can be used to define contributions to the variance from each θ_i by summing the variance and covariance terms involving θ_i,

$$\mathrm{contribution}(\theta_i) = V(\theta_i)\left(\frac{\partial f}{\partial \theta_i}\right)^2 + \sum_{j \neq i} \mathrm{Cov}(\theta_i, \theta_j) \frac{\partial f}{\partial \theta_i} \frac{\partial f}{\partial \theta_j}.$$

The sum of these contributions is the total (approximate) variance of λ^{ES}, and relative contributions can be computed through dividing by this total variance. Contributions for some parameters can become negative when the covariance terms are negative and dominate the variance. A computationally convenient formula to simultaneously calculate all contributions is

$$\mathrm{contribution}(\theta) := \nabla f_{\bar{\theta}} \circ \Sigma_\theta \ \nabla f_{\bar{\theta}},$$

where $\circ$ denotes element-wise multiplication (Hadamard product).

We note that the above definition of contributions follows common practice in LTRE analyses of splitting covariance terms equally between covarying factors. Covariances can however be of importance on their own (Coulson et al., 2005; Doak et al., 2005) and could be studied via a full contributions matrix

$$\mathrm{diag}(\nabla f_{\bar{\theta}}) \ \Sigma_\theta \ \mathrm{diag}(\nabla f_{\bar{\theta}}).$$

We do not pursue this further here.

Koons et al. (2016) treated the θ as the set of all time varying vital rates (e.g. reproduction and survival at different ages) plus the elements of the population structure vectors. To decompose the variance further we can instead think of θ as containing time varying components of the linear predictors that determine the time varying vital rates, plus the population structure. As an example, suppose we model first year survival as a function of population density, a covariate x and a random effect,

$$\mathrm{logit}(\phi_{0,t}) = \mu + \beta x_t + \gamma \| n_t \| + \varepsilon_t,$$

then the time varying components of this linear predictor are $\beta x_t, \gamma \| n_t \|$, and ε_t. If we collect all such terms across all time varying vital rates and add the population structure, λ_t^{ES} is again completely determined by θ and we can use the variance approximation formula to decompose the variance of the realized growth rate into contributions from the terms in the linear predictors. To do this, we need to compute the gradient $\nabla f_{\bar{\theta}}$ and the covariance matrix Σ_θ. The gradient $\nabla f_{\bar{\theta}}$ is usually straightforward (but potentially tedious) to compute as $\lambda_t^{ES} = \| A_t \tilde{n}_t \|$ tends to

contain simple terms (sums of products between vital rates and population structure) that are easy to differentiate (Appendix S3). This gradient is similar to the gradient when the θ are treated as vital rates (Koons et al., 2016) but with the addition that we also need to take the derivative of the inverses of any link function. The covariance matrix Σ_θ can be estimated by the sample covariance matrix of the full θ vector across time. With IPMs, which are typically implemented using MCMC in a Bayesian framework, it is easy to set up computations so that all the elements of θ are directly available and the covariance matrix can then be computed for each posterior iteration to give a posterior distribution of the contributions.

2.3 | Diagnosing the linear approximation

The approximation used to break down variation in λ^{ES} into its contributing components will not work well if there is strong non-linearity in the relationships between the components and the growth rate over the range of variation in the components. Fortunately, the performance of the approximation can be easily checked by comparing the variance of λ^{ES} to its total variation as indicated by the approximation (sum of all its contributions; Caswell, 2001; Koons et al., 2017). This comparison is also useful for diagnosing coding errors or incorrect calculations of derivatives.

2.4 | Measuring contributions of demographic stochasticity

Demographic stochasticity can be included in population models using distributions that describe outcomes of life-history events at the individual level. For instance, annual survival of an individual may be modelled as a Bernoulli trial and, assuming independence and identical rates among individuals in the same stage in the population, the total number of survivors in a life-stage has a binomial distribution.

In this situation, we define the matrix A_t as the expected projection matrix in year t given the environment (and population size) where the expectation is taken over the demographic stochasticity. In other words, we define A_t using the expected vital rates in year t, e.g. the expected survival probability of an age class. The population vector n_{t+1} is then no longer equal to $A_t n_t$ and we define

$$\lambda_t^D = \frac{\| n_{t+1} \| - \| A_t n_t \|}{\| n_t \|},$$

so that

$$\lambda_t = \frac{\| n_{t+1} \|}{\| n_t \|} = \lambda_t^{ES} + \lambda_t^D.$$

The numerator of λ_t^D is the difference between actual population size and the projected population size we would expect from environmental variation alone, and λ_t^D therefore represents growth beyond what is captured by age structure and variation in the environment, i.e. the total combined effect of demographic stochasticity. It can be a complex quantity involving products or sequences of demographic stochasticity from multiple vital rates, but can be implemented by simulating from the distributions representing demographic stochasticity, e.g. within an IPM as we illustrate in the case study below. Note that λ^D unlike λ^{ES} can be both negative and positive but this would be avoided if the decomposition is defined at the log-scale. For large n, λ^D should become small.

We then use

$$\frac{V(\lambda^{ES}) + \mathrm{Cov}(\lambda^{ES}, \lambda^D)}{V(\lambda)}$$

as a measure of the relative contribution of environmental variation and population structure to variation in the realized growth rate, and, correspondingly,

$$\frac{V(\lambda^D) + \mathrm{Cov}(\lambda^D, \lambda^{ES})}{V(\lambda)}$$

for the relative contribution of demographic stochasticity. Covariance terms are included so that the sum of the two relative contributions is 1.

The same idea can also be used to compute contributions from environmental variation and age structure to the overall variation in λ instead of to just λ^{ES}. For this, one can use the same formulas for the contributions as in the previous section but including λ_t^D as one of the components of the parameter vector θ with a corresponding derivative equal to 1, or alternatively modify the contributions to λ^{ES} by adding covariance terms between each of the components and λ^D (see Appendix S3 for an illustration).

2.5 | Contributions to λ^D

It may be of interest to decompose λ^D and compute contributions to its variance. While one could potentially try to decompose it into contributions from each vital rate, as for the decomposition of λ^{ES}, it is not obvious how to do this when vital rates enter A_t as products (but the methods of Hernández et al. (2023) could potentially be employed for this, see Section 3). We instead consider the simpler approach of decomposing λ^D into additive components of $\| A_t n_t \|$. The numerator of λ_t^D, $\| n_{t+1} \| - \| A_t n_t \|$, may be written as a sum of differences between the number of individuals arising as a result of demographic stochasticity and the expected number of individuals from environmental stochasticity alone for each of the additive components, and given the initial stage structure vector n_t. From these differences, contributions to the variance of λ^D can be computed similarly to above (see Appendix S3 for how to do this for the case study below).

2.6 | Case study using transient LTREs with IPMs

The above decompositions can be used in combination with inference via IPMs. We will illustrate this in a case study where we first

compute the contribution of environmental covariates, density dependence and population structure to variation in λ^{ES} as in the previous section, and then separately estimate the relative magnitude of environmental and demographic variation. For the case study, we use field data from 26 years (1993–2018) from a population of wheatears, a migratory bird species wintering in the Sahel region and breeding in an agricultural landscape near Uppsala in Sweden. We use mark-resighting data of birds ringed either as adults or as chicks in the nest, data on reproductive performance and census data on occupied breeding territories to parametrize an age structured population model by combining data in an IPM. The model has two age classes describing the number of young males (1 year old) and the number of males older than 1 year (>1 year) in a pre-breeding census formulation. We chose these two age classes because the species is short-lived and because short-lived birds in general tend to show the most prominent change in vital rates from an age of 1–2 years (e.g. Newton, 1989). We only consider males as they can be categorized as young or older than 1 year in the field based on plumage characteristics (Pärt, 2001), whereas the same female age classes are harder to determine. Details of the wheatear study system and how data are handled and combined in the IPM are provided in Appendix S1, and we focus below on the annual dynamics resulting from the IPM.

2.7 | Annual projection matrix

The basic structure of the environmental annual projection matrix A_t is

$$A_t = \begin{pmatrix} \nu_{1,t} r \psi_t \zeta \phi_{0,t} + \omega_{1,t} & \nu_{2,t} r \psi_t \zeta \phi_{0,t} + \omega_{1,t} \\ \phi_{1,t} + \omega_{2,t} & \phi_{2,t} + \omega_{2,t} \end{pmatrix}.$$

Briefly, $\nu_{1,t}$ and $\nu_{2,t}$ represent the probability of early nest survival from initiation of breeding until chicks are approximately 6 days old for young parents (subscript 1) and parents older than 1 year (subscript 2), and r is the expected number of 6 days old chicks produced per nest. Nestling survival is represented by two parameters: ψ_t is the probability that the nest survives as an entity (i.e. that the nest is not destroyed, for example by predation or adverse weather events) from the time nestlings are 6 days old until 15 days when they fledge, and ζ is the probability of individual nestlings to survive until fledgling given that the nest survives. The parameter $\phi_{0,t}$ represents first year apparent survival probability after fledging and includes the probability that the bird is a male (because chicks cannot be sexed in the field, see Appendix S1), $\phi_{1,t}$ and $\phi_{2,t}$ are apparent annual survival probabilities of young males and males older than 1 year. The survival probabilities include the probability of not emigrating out of the study area. The immigration rates into each of the two age classes, $\omega_{1,t}$ and $\omega_{2,t}$, capture the opposite effect of entry into the population for individuals originating from outside of the study area. A more precise definition of the vital rates is given in Table 1.

Except for r and ζ, which are estimated as fixed among years, the vital rates are modelled via link functions (logistic for survival probabilities and log for immigration rates) as depending on environmental covariates, density dependence and annual random effects. For early nest survival and nestling survival we used local rain and temperature during those stages as covariates, for first year survival after fledging we used breeding population density and rainfall in the wintering area, and for survival of young males and males older than 1 year we used local rainfall and temperature in summer as well as rainfall in the wintering area (Table 1). Further motivation behind the choice of environmental covariates is given in Appendix S1. All covariates were defined at the population level, and therefore are the same for all individuals in a given stage and year, not taking into account the timing of individual breeding events within seasons.

2.8 | Demographic stochasticity

The components of demographic stochasticity enter the IPM naturally in the likelihood for the demographic data as one source of sampling variation. For instance, demographic stochasticity in survival is naturally integrated and accounted for in mark recapture models. Demographic stochasticity can also be included in the population model associated with the census part of the IPM likelihood (e.g. Abadi et al., 2012). We do this starting with the number of individuals in each age class in a given year and sequentially drawing the number of resulting individuals for each vital rate from the respective demographic distributions. These random variables representing demographic stochasticity are modelled with binomial distributions for all survival rates. For the number of chicks we used a categorical distribution and for the number of immigrants into each age class we used Poisson distributions. The expected rates of these distributions are the annual vital rates of the matrix A_t.

As a consequence, the total number of young males in year $t+1$, $n_{1,t+1}$, is the sum of the result of a sequence of binomial and categorical draws involving young males breeding in year t, a sequence of draws involving males older than 1 year breeding in year t and immigration via a $\text{Poisson}\left(\left(n_{1,t}+n_{2,t}\right)\omega_{1,t}\right)$ distributed variable. Likewise, the number of males older than 1 year in year $t+1$, $n_{2,t+1}$, is the sum of a $\text{Binomial}\left(n_{1,t},\phi_{1,t}\right)$, a $\text{Binomial}\left(n_{2,t},\phi_{2,t}\right)$ and a $\text{Poisson}\left(\left(n_{1,t}+n_{2,t}\right)\omega_{2,t}\right)$ distributed variable.

Using these draws λ_t^D can be computed as the difference between $\frac{\| n_{t+1} \|}{\| n_t \|} (= \lambda_t)$ and λ_t^{ES}. We can also compute contributions to the variance in λ^D from its additive components consisting of the number of internal juvenile recruits of 1 year olds from each age class, the number of adult survivors from each age class and the number of immigrants into each age class. More details about how to carry out the calculations in practice are given in Appendix S3.

2.9 | Model fitting details

We formulate the model in a Bayesian framework and therefore need priors for model parameters. For regression coefficients at the logit scale we used normal priors with zero mean and standard

TABLE 1 Overview of the models for environmental variation in vital rates underlying the IPM. Note that we use the same notation for coefficients of the different vital rates but they are included in the IPM as separate parameters (e.g. the slope for rain is different between nestling and first year survival). Random effects are assumed normally distributed and independent among vital rates and with vital rate specific standard deviation.

Vital rate	Notation	Interpretation	Model structure	Covariates
Early nest survival	$\nu_{a,t}$	Probability that a nest of a young ($a = 1$) and a male older than 1 year ($a = 2$) survives until chicks are approximately 6 days old in year t	$\text{logit}(\nu_{a,t}) = \alpha_a + \beta_1 \text{rain}_t + \beta_2 \text{temp}_t + \varepsilon_t$	Mean rainfall and temperature during the incubation period (May 14– June 14)
Fecundity	r	Expected number of 6 days old nestlings given survival of the nest, assumed to be fixed across years	Constant	
Nestling survival (whole nest)	ψ_t	Probability of a nest to survive from the time chicks are 6 days old until fledging (15 days old)	$\text{logit}(\psi_t) = \alpha + \beta_1 \text{rain}_t + \beta_2 \text{temp}_t + \varepsilon_t$	Mean rainfall and temperature during the nestling period (June 2–June 24)
Nestling survival (individual)	ζ	Probability of an individual nestling to survive from an age of 6 days until fledging (15 days old) given that the nest survives	Constant	
First year survival	$\phi_{0,t}$	Probability of a fledgling in year t to be male (the sex of chicks is unknown) and survive and return to establish a territory in year $t + 1$	$\text{logit}(\phi_{0,t}) = \alpha + \beta_1 \text{winter rain}_t + \gamma \lVert n_t \rVert + \varepsilon_t$	Mean rainfall in the wintering area in Sahel during the rain season (June–October), density dependence via total adult population size in the breeding area prior to breeding
Survival of breeding males	$\phi_{a,t}$	Probabilty of a young ($a = 1$) and a male older than 1 year ($a = 2$) with a breeding territory in year t to return and establish a territory in year $t + 1$	$\text{logit}(\phi_{a,t}) = \alpha_a + \beta_{a,1} \text{winter rain}_t + \beta_{a,2} \text{rain}_t + \beta_{a,3} \text{temp}_t + \varepsilon_{a,t}$	Mean rainfall in the wintering area in Sahel durin the rain season (June–October), mean rain and temperature during the nestling period in summer
Immigration	$\omega_{a,t}$	Rates of immigration into young ($a = 1$) males and males older than 1 year ($a = 2$) in year $t + 1$ with respect to the total population in year t	$\log(\omega_{a,t}) = \alpha_a + \varepsilon_{a,t}$	

deviation 1.5 for intercepts and 1 for covariate slopes (Northrup & Gerber, 2018). We used uniform priors over (0, 1) for detection probabilities and for ζ. For the categorical distribution of number of chicks in the nest we used a Dirichlet prior with parameter 1 for all eight categories (representing 1–8 chicks in the nest), yielding a uniform prior over the probability vector.

For vital rates for which there are no direct observed data, typically immigration as in our case, contributions tend to get inflated when temporal random effects for them are modelled (Paquet et al., 2021). To reduce this effect we put exponential shrinkage priors (rate = 20) on the random effect standard deviations (for all vital rate random effects, not only immigration). These priors aim to reduce model complexity (Simpson et al., 2017) by shrinking variation toward zero. As a consequence, a small posterior random effect variance does not necessarily mean that the variation in the parameter is small, but simply that there is no evidence of strong variation.

We also put a shrinkage prior on the intercepts for immigration (rate = 10) as we do not have direct data on immigration, which might lead to unstable estimation of this parameter.

The IPM was implemented in NIMBLE (de Valpine et al., 2016) using four MCMC chains, each with 21,000 iterations and discarding the first 1000 iterations (code available at github). For each iteration of the MCMC output we computed contributions from each component of the linear predictors of the vital rates, age structure and demographic stochasticity, to yield the posterior distribution of the contributions. Convergence of the MCMC was assessed using the R-hat statistic on the 4 chains. These were all below 1.03.

Model fit was assessed by posterior predictive *p*-values (Appendix S2). The fit was deemed acceptable for the aspects of the model that we investigated.

In addition to the main model we considered an alternative with a different specification of nestling survival. The alternative model assumed that variation in nestling survival rates was due to deaths of individual young in the nest, as opposed to total nest failure in the main model (see Appendices S1 and S2 for further discussion).

The age-structure vector in our case has two components that sum to 1, so that there is only one degree of freedom in its variation. We therefore parameterized λ_t^{ES} as a function of $\tilde{n}_{1,t}$ only (i.e. with $\tilde{n}_{2,t}$ replaced by $1 - \tilde{n}_{1,t}$) when computing the gradient and contributions.

2.10 | Results of case study

The population declined over the study period with a marked variation in annual growth rates (Figure 1). Decomposing the variance in the realized growth rate without demographic stochasticity (λ^{ES}) into contributions from vital rates (similarly to Koons et al., 2016, 2017) suggests that most of the variation comes from first year survival, and with seemingly smaller contributions from survival of males older than 1 year, young males and nestlings (Figure 2). Early nest survival and immigration both have small contributions, and variation in age structure contributed almost nothing to variation in growth.

Breaking the contributions down into environmental components affecting the vital rates suggests that random effects and winter rain for first year survival, and summer temperature for survival of males older than 1 year provide the largest contributions to environmental variation in the growth rate (Figure 3). The effects of these two rain and temperature covariates, as well as the

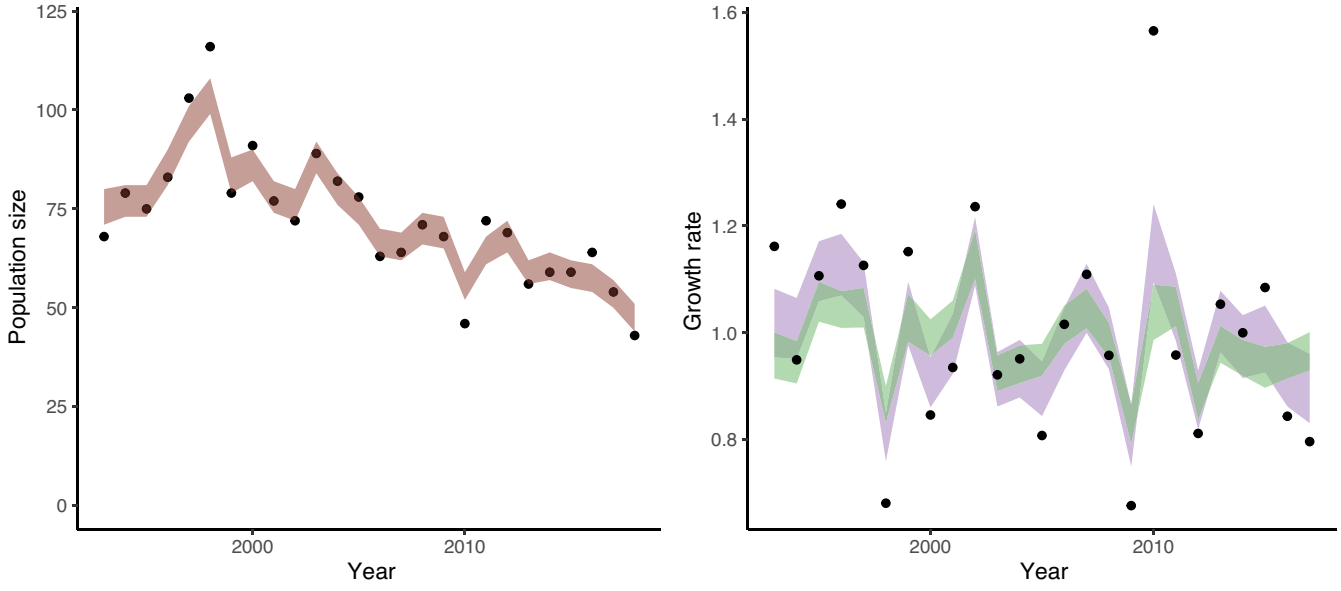

FIGURE 1 Left panel: Observed (points) and estimated (shaded area, showing 50% credible intervals) population size over the study period. Right panel: Observed (points) and estimated (shaded areas, showing 50% credible intervals) annual growth rates. The green shaded area shows estimated annual growth rates including environmental variation and variation in age structure (i.e. λ^{ES}), the purple shaded area shows estimated growth rate also including demographic stochasticity (i.e. $\lambda^{ES} + \lambda^{D}$).

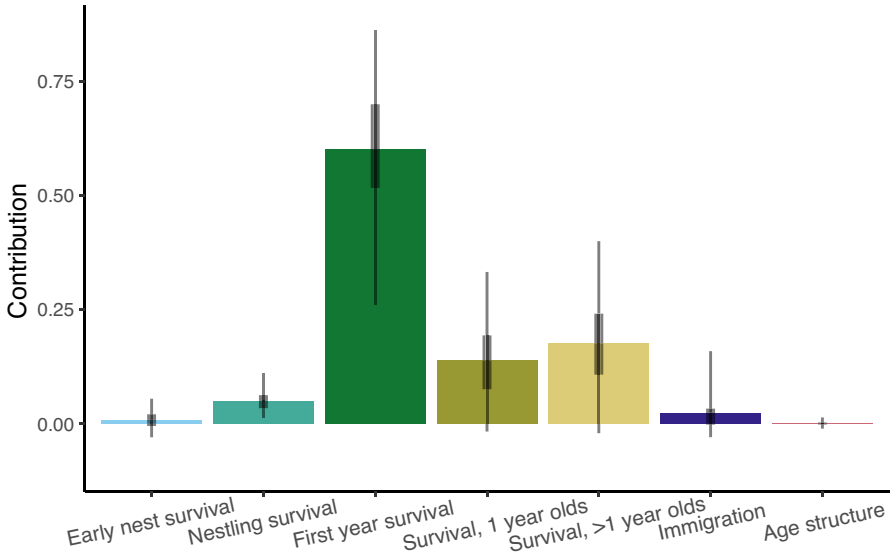

FIGURE 2 Total relative contributions to environmental variance in the realized growth rate for each vital rate (summed across all linear predictor components of the vital rates). Error bars show 50% (thick) and 95% (thin) credible intervals.

contributions, are however uncertain (Figure 4). There is a clearer effect for summer temperature on nestling survival, but the resulting contribution to variation in growth is small.

Alternatively, we may compute total contributions of different groups of variables that may act across different vital rates. For example, Figure 5 shows total contributions of weather, density, random effects and population structure to the variance in the realized growth rate, indicating that roughly equal portions of the variance are due to weather and random effects in the model. The weather contributions were computed by summing contributions from all temperature and rainfall covariates across all vital rates, and the random effect contributions by summing all random effects components across all vital rates (including immigration).

Comparing the actual variance of λ^{ES} to the approximated variance (i.e. the sum of all contributions) shows that the approximation slightly underestimated the actual variance with a relative error of −1% on average over the posterior distribution, but with larger errors for some posterior draws (95% CI: −16%–14%).

The above results show contributions to environmental variation in growth only. If we consider the population across the censused area, which has around 50–120 individual males per year, demographic stochasticity accounts for a large portion of the variance in the realized growth rate. Specifically the contribution of demographic stochasticity via λ^{D} is ca 56% (95% CI: 31%–82%), while the remaining contribution is due to variation in λ^{ES}. The contributions to λ^{D} are uncertain and split among internal juvenile recruitment, survival and immigration of the two age classes (Figure 6).

In the alternative model where variation in nestling survival is assumed to be due to death of individual chicks instead of total nest failure (Appendix S2), there is a large contribution of nestling survival to variation in growth, and a smaller contribution from first year survival compared to the main model (Figure S1). In this model, the contributions from temperature and rainfall via nestling survival are also larger (Figure S2). Because distinguishing the two models is difficult (Appendix S2), it is not fully clear during which part of the time period from the ringing of chicks to their return the following year that some of the variation contributing to variation in growth occurs. The approximation of contributions to λ^{ES} performed less well than for the main model with an average relative error of −6%.

3 | DISCUSSION

Transient LTREs have previously been used mainly to decompose variance in realized growth rates into contributions from vital rates and age-structure, even when environmental predictors have been included in models (e.g. Canonne et al., 2023; Nater et al., 2022). We show how transient LTREs can be used to also decompose the variation in vital rates into contributions from environmental factors and density dependence, and to assess the overall contribution of environmental versus demographic stochasticity, two conceptual extensions of the approach of Koons et al. (2016).

3.1 | Estimating contributions

The decomposition of environmental variation relies on approximating the environmental realized growth rate using a first order Taylor expansion, which may not be accurate if there is strong environmental variation or strong non-linearity in the response to the environment. In our case study the average relative error was a modest −1%, but was higher over parts of the posterior distribution and also higher for the alternative model. Other decompositions to try to reduce error have been proposed. Rees and Ellner (2009) suggested LTREs of the realized growth rate for integral projection models that rely on multiple regression of growth rates against vital rates for simulated population dynamics. This approach has been extended to LTREs of environmental factors determining the vital rates, also for integral projection models (Maldonado-Chaparro et al., 2018). It

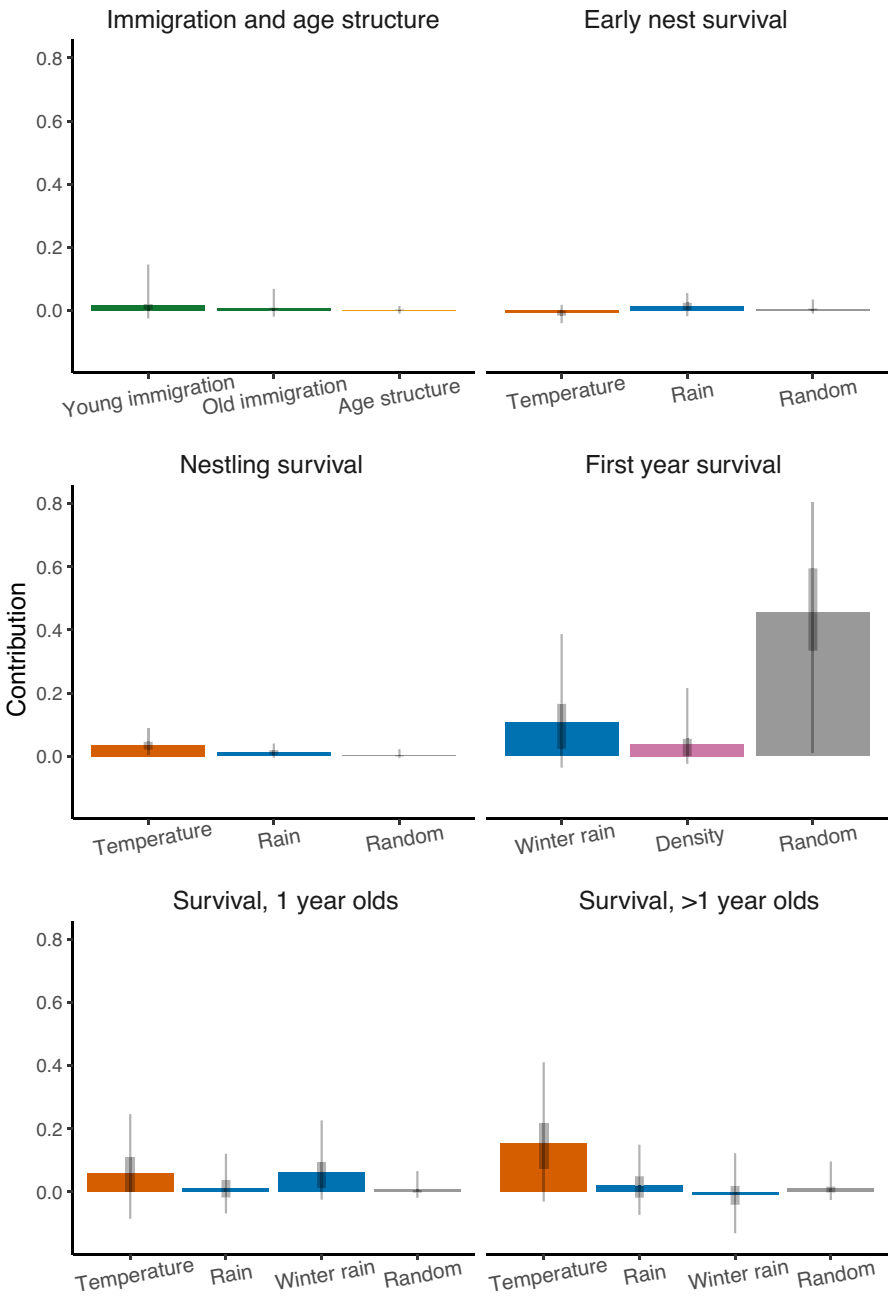

FIGURE 3 Relative contributions (summing to 1) to environmental variation in the realized growth rate from all linear predictor components and vital rates. Error bars show 50% (thick) and 95% (thin) credible intervals.

differs from the approach taken here in that a simulation scheme for hypothetical environmental variables, which assumes stationarity in the environment, as well as a regression model to analyse the simulated growth rates need to be set up. In contrast, Taylor approximation-based LTREs are directly derived from the model and no design choices are necessary in the calculation of contributions. Another difference is that while we estimate only direct effects on the growth rate, Maldonado-Chaparro et al. (2018) aim to also estimate lagged effects of environmental variables. Such lagged effects would appear in the age structure contributions of our approach.

Another possibility is to use functional decompositions (Hooker, 2007) as a basis for LTREs. Hernández et al. (2023) proposed this approach and used it to decompose differences in the asymptotic growth rate between treatments. It could at least in theory be used to approximate the variance in realized growth rates, potentially including both λ^{ES} and λ^{D}, to an arbitrary degree of precision by increasing the order of the functional expansion, but in practice computation time and interpretation will be limiting factors (Hernández et al., 2023).

It is unclear to us when and if these alternative decompositions would perform better than the Taylor approximation-based LTREs. We suggest that the more direct Taylor based or functional decomposition approaches could be used in first attempts to compute contributions from environmental variables. In cases where the performance turns out to be poor, a simulation approach (Maldonado-Chaparro et al., 2018) could be considered.

To measure contributions from demographic stochasticity, we compare the growth rate when random outcomes from all the model

components that represent demographic stochasticity are included to the expected growth rates when these components are fixed at their annual means. The relative effect of the demographic stochasticity components will decrease with population size and hence the relative contribution of demographic stochasticity will depend on the size of the population that is considered. In an IPM with census data, an obvious choice is to estimate the contribution of demographic stochasticity for the population that is being censused as we have done in our case study. However, the contribution of demographic stochasticity could be predicted more generally by simulating the outcomes of demographic events for a population of any given initial size.

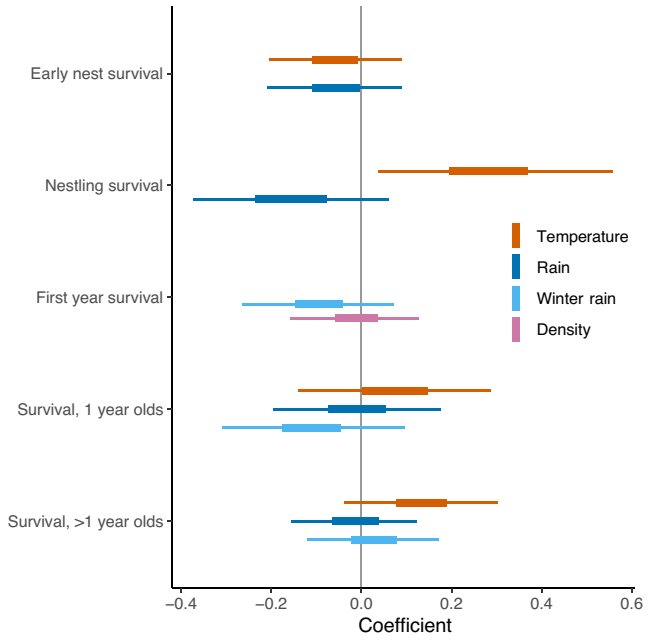

FIGURE 4 Estimated slopes for all environmental covariates on vital rates. Error bars show 50% (thick) and 95% (thin) credible intervals.

3.2 | Case study

For the wheatear population model, an LTRE decomposition into vital rate contributions suggests that environmental variation in annual growth rates mainly comes from variation in first year survival after fledging and in survival of males older than 1 year (Figure 2). Further decomposing these contributions into components from environmental variables shows that the contribution from first year survival is mainly linked to unexplained random variation while the contribution from survival of males older than 1 year is related to summer temperatures. In total, around half of the environmental variation in growth were explained by weather covariates while the other half came from the unexplained random components. Another new aspect of our IPM analysis is that we also quantify the magnitude of demographic stochasticity, and a large portion of the variance in the realized growth rate seems to come from this component.

The importance of first year and adult survival is partly in agreement with a previous transient LTRE analysis of vital rates in this population using a different model (Paquet et al., 2019). Our results are also partly compatible with previous analyses of weather variables in the wheatear population, conducted at an individual level rather than at the population level adopted here. These suggested, among other things, that rainfall during the nestling period reduced fledging success and that temperature increased it (Öberg et al., 2015). Our results point in the same direction although the negative effect of rainfall was uncertain in the main model. The implications on variation in population growth however was strongly dependent on the specification of the nestling survival model. In the main model the contribution from these weather effects via nestling survival were very small, but substantial in the alternative model. This shows how seemingly innocuous model specification choices, in this case whether variation in nestling survival was due to complete nest failure or to death of individual chicks, can sometimes lead to substantial differences in contributions.

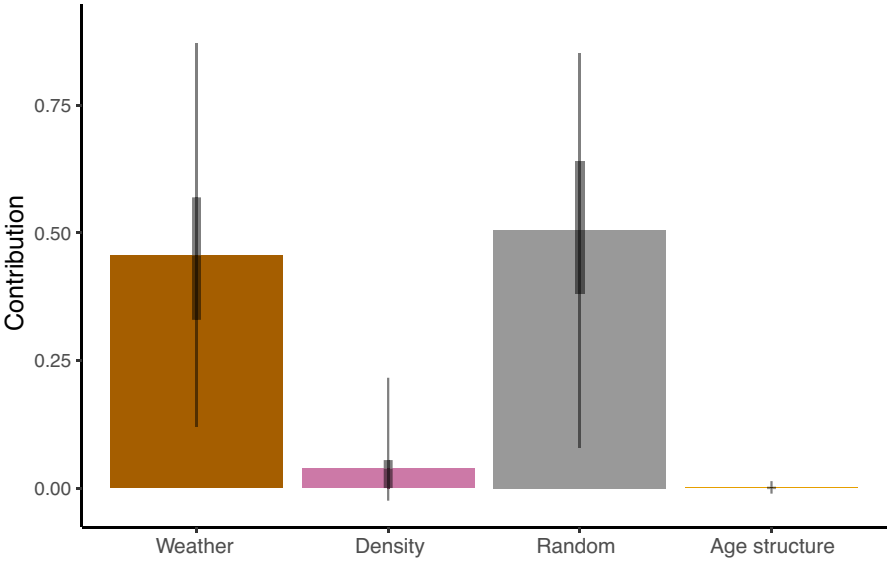

FIGURE 5 Relative contributions from weather (rainfall and temperature), population density, random effects (including for immigration) and age structure to environmental variance in realized growth. Error bars show 50% (thick) and 95% (thin) credible intervals.

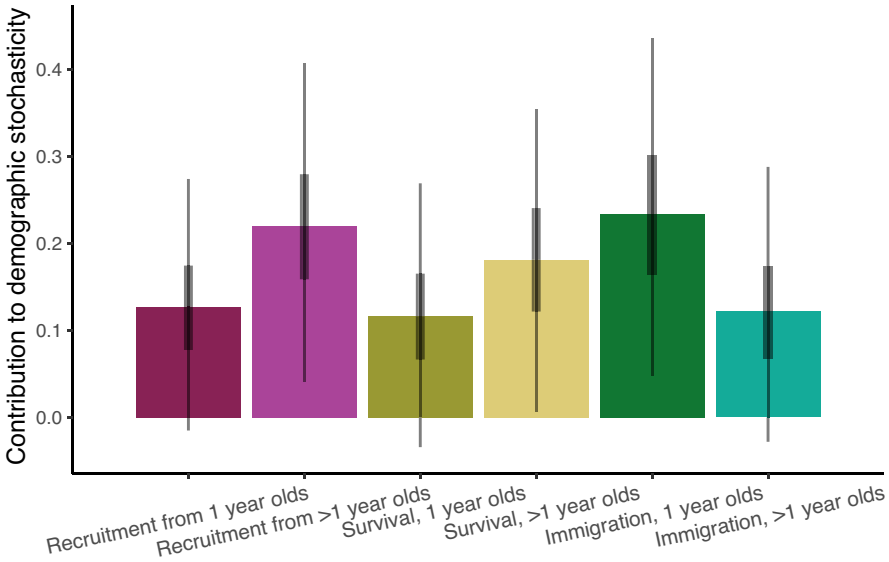

FIGURE 6 Relative contributions from internal juvenile recruitment, survival and immigration of each age class to variance in λ^D. Error bars show 50% (thick) and 95% (thin) credible intervals.

Similarly to Paquet et al. (2019), the contribution from age structure was small. This is a result both of limited age differences in vital rates and limited variation in age structure across years. Including more age classes would be unlikely to affect this result as the proportion of individuals in higher age classes decreases rapidly for short lived species, and the main age related changes in vital rates tend to occur in the first 2 years for short-lived birds (Newton, 1989).

The large contribution from demographic stochasticity (56%) may seem high, but is not unreasonable for a population of this size (100 males, cf. Lande et al., 2003; Steiner et al., 2021). Nevertheless, estimating environmental variability in demographic rates from study populations of limited size is a challenge because its signals can be obscured by demographic stochasticity, even for long term studies (Ross & Weegman, 2022). This may partly explain the large uncertainty often seen in estimated contributions, here and in other studies.

In contrast to several other studies (Millon et al., 2019; Nater et al., 2022; e.g. Weegman et al., 2017), including the previous IPM study on wheatears (Paquet et al., 2019), our results suggest limited contribution of immigration to annual variation in growth rates. We believe this is mainly a consequence of our use of penalized complexity priors (Simpson et al., 2017) for random effects variances. Using an uninformative weak prior for variation in immigration will often result in a large contribution because direct information about immigration is typically missing (Paquet et al., 2021) and estimated variation is dependent on the prior. Penalized complexity priors are a convenient way of mitigating this effect by allowing some variation in immigration rates but not a lot more than is indicated by the data (Simpson et al., 2017).

A flatter prior on the standard deviation of the random components would also likely have led to a larger posterior mean relative contribution of environmental stochasticity, especially via immigration. Thereby the mean relative contribution of environmental stochasticity would have been inflated, but at the same time larger uncertainty in the estimate of the contribution would be expected.

4 | CONCLUSIONS

LTRE analyses of realized growth rates have been used to shed light on how variation in vital rates over a study period contribute to population change. The methods illustrated here provide a means of assessing how these contributions are mediated by lower level drivers, including environmental factors, intraspecific density dependence and conceivably interspecific density dependence, and additionally to determine contributions from demographic stochasticity. They can give us a more complete picture of the different paths along which a population model moderates fundamental sources of variation into variation in population growth.

AUTHOR CONTRIBUTIONS

Jonas Knape and Matthieu Paquet conceived the initial idea for the study. Jonas Knape designed methods and analysed data, with input from all authors, and wrote the original draft. Tomas Pärt initiated the field study, Debora Arlt and Tomas Pärt led the study and curated data. Debora Arlt extracted initial data for analysis. All authors contributed to revisions of the text.

ACKNOWLEDGEMENTS

We thank David Koons, an anonymous reviewer and the associate editor for helpful comments and suggestions.

CONFLICT IF INTEREST STATEMENT

The authors have no conflict of interest to declare.

DATA AVAILABILITY STATEMENT

Data are available from the Dryad Digital Repository https://doi.org/10.5061/dryad.98sf7m0pj (Knape et al., 2023b), and code from Zenodo https://doi.org/10.5281/zenodo.8116971 (Knape et al., 2023a). Both code and data are also available at github, https://github.com/jknape/variance-decomp.

ORCID

Jonas Knape https://orcid.org/0000-0002-8012-5131
Matthieu Paquet https://orcid.org/0000-0003-1182-2299
Debora Arlt https://orcid.org/0000-0003-0874-4250
Ineta Kačergytė https://orcid.org/0000-0003-4756-8253
Tomas Pärt https://orcid.org/0000-0001-7388-6672

REFERENCES

Abadi, F., Gimenez, O., Jakober, H., Stauber, W., Arlettaz, R., & Schaub, M. (2012). Estimating the strength of density dependence in the presence of observation errors using integrated population models. *Ecological Modelling*, *242*, 1–9. https://doi.org/10.1016/j.ecolmodel.2012.05.007

Arlt, D., Forslund, P., Jeppsson, T., & Pärt, T. (2008). Habitat-specific population growth of a farmland bird. *PLoS ONE*, *3*(8), e3006. https://doi.org/10.1371/journal.pone.0003006

Arlt, D., Olsson, P., Fox, J. W., Low, M., & Pärt, T. (2015). Prolonged stopover duration characterises migration strategy and constraints of a long-distance migrant songbird. *Animal Migration*, *2*(1), 47–62. https://doi.org/10.1515/ami-2015-0002

Arlt, D., & Pärt, T. (2017). Marked reduction in demographic rates and reduced fitness advantage for early breeding is not linked to reduced thermal matching of breeding time. *Ecology and Evolution*, *7*, 10782–10796. https://doi.org/10.1002/ece3.3603

Besbeas, P., Freeman, S. N., & Morgan, B. J. T. (2005). The potential of integrated population modelling. *Australian & New Zealand Journal of Statistics*, *47*(1), 35–48. https://doi.org/10.1111/j.1467-842X.2005.00370.x

Brown, D., Alexander, N. D. E., Marrs, R. W., & Albon, S. (1993). Structured accounting of the variance of demographic change. *Journal of Animal Ecology*, *62*(3), 490–502. https://doi.org/10.2307/5198

Canonne, C., Bernard-Laurent, A., Souchay, G., Perrot, C., & Besnard, A. (2023). Contrasted impacts of weather conditions in species sensitive to both survival and fecundity: A montane bird case study. *Ecology*, *104*(2), e3932. https://doi.org/10.1002/ecy.3932

Caswell, H. (1989). Analysis of life table response experiments I. Decomposition of effects on population growth rate. *Ecological Modelling*, *46*(3), 221–237. https://doi.org/10.1016/0304-3800(89)90019-7

Caswell, H. (2001). *Matrix population models* (2nd ed.). Sinauer Associates.

Clark-Wolf, T. J., Dee Boersma, P., Rebstock, G. A., & Abrahms, B. (2023). Climate presses and pulses mediate the decline of a migratory predator. *Proceedings of the National Academy of Sciences of the United States of America*, *120*(3), e2209821120. https://doi.org/10.1073/pnas.2209821120

Cohen, J. E. (1977). Ergodicity of age structure in populations with Markovian vital rates, III: Finite-state moments and growth rate; an illustration. *Advances in Applied Probability*, *9*(3), 462–475. https://doi.org/10.2307/1426109

Coulson, T., Gaillard, J.-M., & Festa-Bianchet, M. (2005). Decomposing the variation in population growth into contributions from multiple demographic rates. *Journal of Animal Ecology*, *74*(4), 789–801. https://www.jstor.org/stable/3505459

Cramp, S. (1988). *Handbook of the birds of Europe, the Middle East and North Africa. The birds of the Western palearctic. Vol. 5: Tyrant flycatchers to thrushes*. Oxford University Press.

Davison, R., Nicolè, F., Jacquemyn, H., & Tuljapurkar, S. (2013). Contributions of covariance: Decomposing the components of stochastic population growth in *Cypripedium calceolus*. *The American Naturalist*, *181*(3), 410–420. https://doi.org/10.1086/669155

de Valpine, P., Turek, D., Paciorek, C. J., Anderson-Bergman, C., Lang, D. T., & Bodik, R. (2016). Programming with models: Writing statistical algorithms for general model structures with NIMBLE. *Journal of Computational and Graphical Statistics*, 1–28. https://doi.org/10.1080/10618600.2016.1172487

Doak, D. F., Morris, W. F., Pfister, C., Kendall, B. E., & Bruna, E. M. (2005). Correctly estimating how environmental stochasticity influences fitness and population growth. *The American Naturalist*, *166*(1), E14–E21. https://doi.org/10.1086/430642

Engen, S., Bakke, Ø., & Islam, A. (1998). Demographic and environmental stochasticity-concepts and definitions. *Biometrics*, *54*(3), 840–846. http://www.jstor.org/stable/2533838

Hernández, C. M., Ellner, S. P., Adler, P. B., Hooker, G., & Snyder, R. E. (2023). An exact version of Life Table Response Experiment analysis, and the R package exactLTRE. *Methods in Ecology and Evolution*, *14*(3), 939–951. https://doi.org/10.1111/2041-210X.14065

Hooker, G. (2007). Generalized functional ANOVA diagnostics for high-dimensional functions of dependent variables. *Journal of Computational and Graphical Statistics*, *16*(3), 709–732. https://doi.org/10.1198/106186007X237892

JISAO. (2018). *Sahel precipitation index* [data set]. https://doi.org/10.6069/H5MW2F2Q

Knape, J., Paquet, M., Arlt, D., Kačergyté, I., & Pärt, T. (2023a). Data from: Partitioning variance in population growth for models with environmental and demographic stochasticity. *Zenodo*, https://doi.org/10.5281/zenodo.8116971

Knape, J., Paquet, M., Arlt, D., Kačergyté, I., & Pärt, T. (2023b). Data from: Partitioning variance in population growth for models with environmental and demographic stochasticity [data set]. *Dryad Digital Repository*, https://doi.org/10.5061/dryad.98sf7m0pj

Koons, D. N., Arnold, T. W., & Schaub, M. (2017). Understanding the demographic drivers of realized population growth rates. *Ecological Applications*, *27*(7), 2102–2115. https://doi.org/10.1002/eap.1594

Koons, D. N., Iles, D. T., Schaub, M., & Caswell, H. (2016). A life-history perspective on the demographic drivers of structured population dynamics in changing environments. *Ecology Letters*, *19*(9), 1023–1031. https://doi.org/10.1111/ele.12628

Lande, R., Engen, S., & SÆther, B.-E. (2003). Demographic and environmental stochasticity. In R. Lande, S. Engen, & B.-E. Saether (Eds.), *Stochastic population dynamics in ecology and conservation* (pp. 1–24). Oxford University Press. https://doi.org/10.1093/acprof:oso/9780198525257.003.0001

Low, M., Arlt, D., Eggers, S., & Pärt, T. (2010). Habitat-specific differences in adult survival rates and its links to parental workload and on-nest predation. *Journal of Animal Ecology*, *79*(1), 214–224. https://doi.org/10.1111/j.1365-2656.2009.01595.x

Maldonado-Chaparro, A. A., Blumstein, D. T., Armitage, K. B., & Childs, D. Z. (2018). Transient LTRE analysis reveals the demographic and trait-mediated processes that buffer population growth. *Ecology Letters*, *21*(11), 1693–1703. https://doi.org/10.1111/ele.13148

Millon, A., Lambin, X., Devillard, S., & Schaub, M. (2019). Quantifying the contribution of immigration to population dynamics: A review of methods, evidence and perspectives in birds and mammals. *Biological Reviews*, *94*(6), 2049–2067. https://doi.org/10.1111/brv.12549

Nater, C., Burgess, M., Coffey, P., Harris, B., Lander, F., Price, D., Reed, M., & Robinson, R. (2022). Spatial consistency in drivers of population dynamics of a declining migratory bird. *Journal of Animal Ecology*, *92*, 97–111. https://doi.org/10.1111/1365-2656.13834

Newton, I. (1989). *Lifetime reproduction in birds*. Academic.

Northrup, J. M., & Gerber, B. D. (2018). A comment on priors for Bayesian occupancy models. *PLoS ONE*, *13*(2), e0192819. https://doi.org/10.1371/journal.pone.0192819

Öberg, M., Arlt, D., Pärt, T., Laugen, A. T., Eggers, S., & Low, M. (2015). Rainfall during parental care reduces reproductive and survival components of fitness in a passerine bird. *Ecology and Evolution*, *5*(2), 345–356. https://doi.org/10.1002/ece3.1345

Paquet, M., Arlt, D., Knape, J., Low, M., Forslund, P., & Pärt, T. (2019). Quantifying the links between land use and population growth rate

in a declining farmland bird. *Ecology and Evolution*, *9*(2), 868–879. https://doi.org/10.1002/ece3.4766

Paquet, M., Knape, J., Arlt, D., Forslund, P., Pärt, T., Flagstad, Ø., Jones, C. G., Nicoll, M. A. C., Norris, K., Pemberton, J. M., Sand, H., Svensson, L., Tatayah, V., Wabakken, P., Wikenros, C., Åkesson, M., & Low, M. (2021). Integrated population models poorly estimate the demographic contribution of immigration. *Methods in Ecology and Evolution*, *12*(10), 1899–1910. https://doi.org/10.1111/2041-210X.13667

Pärt, T. (2001). The effects of territory quality on age-dependent reproductive performance in the northern wheatear, *Oenanthe oenanthe*. *Animal Behaviour*, *62*(2), 379–388. https://doi.org/10.1006/anbe.2001.1754

Plard, F., Fay, R., Kéry, M., Cohas, A., & Schaub, M. (2019). Integrated population models: Powerful methods to embed individual processes in population dynamics models. *Ecology*, e02715. https://doi.org/10.1002/ecy.2715

Rees, M., & Ellner, S. P. (2009). Integral projection models for populations in temporally varying environments. *Ecological Monographs*, *79*(4), 575–594. https://doi.org/10.1890/08-1474.1

Ross, B. E., & Weegman, M. D. (2022). Relative effects of sample size, detection probability, and study duration on estimation in integrated population models. *Ecological Applications*, *32*(8), e2686. https://doi.org/10.1002/eap.2686

Schaub, M., & Kéry, M. (2021). *Integrated population models: Theory and ecological applications with R and JAGS* (1st ed.). Academic Press.

Simpson, D., Rue, H., Riebler, A., Martins, T. G., & Sørbye, S. H. (2017). Penalising model component complexity: A principled, practical approach to constructing priors. *Statistical Science*, *32*(1), 1–28. https://doi.org/10.1214/16-STS576

Steiner, U. K., Tuljapurkar, S., & Roach, D. A. (2021). Quantifying the effect of genetic, environmental and individual demographic stochastic variability for population dynamics in *Plantago lanceolata*. *Scientific Reports*, *11*(1), Article 23174. https://doi.org/10.1038/s41598-021-02468-9

Ver Hoef, J. M. (2012). Who invented the Delta method? *The American Statistician*, *66*(2), 124–127. https://doi.org/10.1080/00031305.2012.687494

Weegman, M. D., Arnold, T. W., Dawson, R. D., Winkler, D. W., & Clark, R. G. (2017). Integrated population models reveal local weather conditions are the key drivers of population dynamics in an aerial insectivore. *Oecologia*, *185*(1), 119–130. https://doi.org/10.1007/s00442-017-3890-8

Zhao, Q., Heath-Acre, K., Collins, D., Conway, W., & Weegman, M. D. (2021). Integrated population modelling reveals potential drivers of demography from partially aligned data: A case study of snowy plover declines under human stressors. *PeerJ*, *9*, e12475. https://doi.org/10.7717/peerj.12475

SUPPORTING INFORMATION

Additional supporting information can be found online in the Supporting Information section at the end of this article.

Appendix S1: IPM details.

Appendix S2: Goodness of fit and an alternative model.

Appendix S3: Tutorial.

How to cite this article: Knape, J., Paquet, M., Arlt, D., Kačergytė, I., & Pärt, T. (2023). Partitioning variance in population growth for models with environmental and demographic stochasticity. *Journal of Animal Ecology*, *92*, 1979–1991. https://doi.org/10.1111/1365-2656.13990